# Advancements of Global Navigation Satellite System radio occultation retrieval in the upper stratosphere for optimal climate monitoring utility

A. Gobiet and G. Kirchengast

Institute for Geophysics, Astrophysics, and Meteorology, University of Graz, Graz, Austria

Received 10 June 2004; revised 10 September 2004; accepted 29 October 2004; published 29 December 2004.

[1] Global Navigation Satellite System–based radio occultation (RO) measurements promise to become a valuable observational basis for climate research, numerical weather prediction, and atmospheric process studies, thanks to their unique combination of global coverage, high accuracy and vertical resolution, and long-term stability. Concerning the quality of the RO-derived atmospheric profiles, performance simulation studies and first data analysis results from the current CHAMP satellite mission are encouraging but also reveal weaknesses of present RO retrieval chains at high altitudes (above 30 km). This study aims at providing, first, understanding of these weaknesses and, second, mitigation by an advanced retrieval scheme. We first evaluated present state-of-the-art high-altitude RO retrieval algorithms. We found clear superiority for using statistical optimization involving background information over using exponential extrapolation and a sensitivity of RO retrieval products to biases in background information calling for sensible bias mitigation. Exploiting these findings, an advanced high-altitude retrieval scheme is presented, which focuses on minimizing residual retrieval biases in the upper stratosphere and thereby on optimizing the climate monitoring utility of retrieved profiles. Applied to a large ensemble of simulated occultation events, the advanced scheme proved to be effective. The scheme is currently under evaluation with real data from the CHAMP mission. It will then serve as part of a processing chain generating RO-based global climatologies of refractivity, geopotential height, temperature, and humidity based on RO data from CHAMP, SAC-C, GRACE and other future satellites carrying RO instruments. *INDEX TERMS:* 1640 Global Change: Remote sensing; 1610 Global Change: Atmosphere (0315, 0325); 1694 Global Change: Instruments and techniques; 3360 Meteorology and Atmospheric Dynamics: Remote sensing; *KEYWORDS:* radio occultation, statistical optimization, retrieval

**Citation:** Gobiet, A., and G. Kirchengast (2004), Advancements of Global Navigation Satellite System radio occultation retrieval in the upper stratosphere for optimal climate monitoring utility, *J. Geophys. Res.*, *109*, D24110, doi:10.1029/2004JD005117.

## 1. Introduction

[2] Detecting and observing changes and variability in the global climate is one of the most important challenges in atmospheric sciences over the coming decades since there exists evidence and concern that the Earth's climate is increasingly influenced by human activities [e.g., *Intergovernmental Panel on Climate Change*, 2001]. Global warming and climate change in general is not only a scientific but also a societal-political topic, which makes it especially important to establish reliable and stable long-term records of key climate variables such as atmospheric temperature. Since long-term in situ measurements face, especially on global scale, many difficulties like calibration, temporal and spatial coverage, and high costs, satellite-borne remote sensing techniques are desirable. However, many satellite-derived data records are degraded by problems like instrument and orbit changes, calibration problems, instrument drifts, and lacking vertical resolution [*Anthes et al.*, 2000]. The Global Navigation Satellite System (GNSS) radio occultation (RO) technique solves many of these problems. It was originally developed and successfully applied to study planetary atmospheres [e.g., *Fjeldbo et al.*, 1971]. The application to Earth's atmosphere became possible with the advent of the U.S. Global Positioning System (GPS) in the early 1980s [*Yunck et al.*, 2000]. Together with the Russian Global Navigation Satellite System and the emerging European GALILEO system, there is now a multitude of transmitter platforms available to be used for sounding Earth's atmosphere with high temporal and spatial resolution. Figure 1 schematically depicts the GNSS RO geometry on Earth. The first suggestions to apply the RO technique to the Earth's atmosphere go back to the 1960s [*Fishbach*, 1965; *Lusignan et al.*, 1969], but the potential of the method was not clearly recognized until the late 1980s [*Gurvich and Krasil'nikova*, 1987; *Yunck et al.*, 1988]. The


0148-0227/04/2004JD005117$09.00

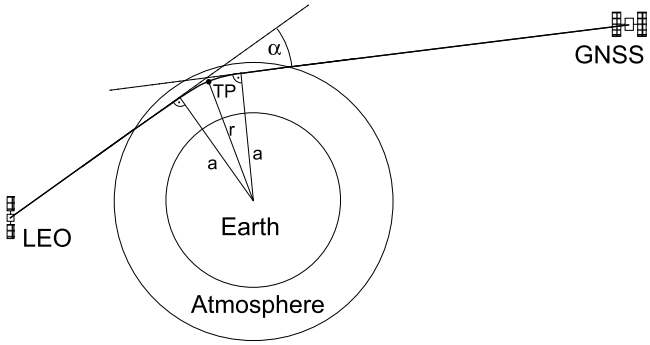


**Figure 1.** Radio occultation geometry [after *Foelsche*, 1999]. LEO is the receiving satellite in low Earth orbit, *a* is impact parameter, $\alpha$ is bending angle, TP is tangent point, and *r* is distance of TP from the center of refraction.

successful "proof-of-concept" experiment GPS/Meteorology (GPS/MET) (1995–1997) demonstrated the unique properties and performance of RO measurements applied to the Earth's atmosphere [*Ware et al.*, 1996; *Kursinski et al.*, 1996; *Rocken et al.*, 1997; *Steiner et al.*, 1999]: high vertical resolution (0.5–1.5 km), high accuracy (<1 K in the upper troposphere and lower stratosphere), all-weather capability, and the global coverage. This confirmed that RO data can play a significant role in atmospheric process studies and numerical weather prediction (NWP) in the near future. Additionally, and potentially most valuable, the expected long-term stability of the method (<0.1 K drift per decade) suggests it as an ideal tool for global climate monitoring and the improvement of climate models [e.g., *Anthes et al.*, 2000; *Kirchengast et al.*, 2000; *Leroy and North*, 2000; *Steiner et al.*, 2001].

[3] The first opportunity for realizing multiyear global RO-based climatologies is provided by the German/U.S. CHAMP research satellite, which was launched on 15 July 2000 into low Earth orbit (LEO) and almost continuously provides ~250 globally distributed occultation events per day from which ~170 quality approved atmospheric profiles can be derived since late 2001 [*Wickert et al.*, 2001, 2004]. Sampling error studies by *Foelsche et al.* [2003] showed that even with one single GPS RO receiver such as on CHAMP, accurate global season-to-season temperature climatologies resolving large horizontal scales >1000 km can be achieved. Higher temporal and spatial resolution can be reached by adding RO data from the Argentine/U.S. SAC-C satellite, providing data since July 2001, and the U.S./German twin satellites GRACE, which are expected to provide RO data from late 2004. Further future perspectives still within this decade include the MetOp weather satellite series, which will carry the GNSS Receiver for Atmospheric Sounding (GRAS, first launch scheduled 2005 [*Edwards and Pawlak*, 2000; *Loiselet et al.*, 2000; *Silvestrin et al.*, 2000]), the German TerraSAR-X satellite (launch scheduled 2005), the U.S./Taiwan COSMIC mission, consisting of six microsatellites carrying GPS RO receivers (launch scheduled 2005 [*Rocken et al.*, 2000]), and the Brazilian EQUARS satellite (launch scheduled 2006).

[4] We aim at using the complete CHAMP and SAC-C RO data flow (and GRACE and later sensor data, as soon as available) for global climate monitoring via refractivity, geopotential height, temperature, and humidity fields. The respective RO data processing system for climate monitoring is currently under development at Institute for Geophysics, Astrophysics, and Meteorology (IGAM).

[5] First retrieval results from the CHAMP mission [*Wickert et al.*, 2001] show a good agreement with colocated European Centre for Medium-Range Weather Forecasts (ECMWF) analyses in the lower stratosphere (temperature bias <0.5 K between 12 and 20 km). However, above 20 km the errors increase significantly. *Wickert et al.* [2001] state that for applications such as climate monitoring, the retrieval scheme has to be improved and the occurrence of biases at stratospheric heights has to be investigated. In the more recently published version 04 of the operational CHAMP retrieval the middle/upper stratosphere temperature differences compared to ECMWF analysis and radiosonde data were further reduced by introducing ECMWF data as background information into the retrieval [*Wickert et al.*, 2004].

[6] First results from a currently ongoing RO climate monitoring system simulation project designed to test the climate change detection capability of GNSS occultation sensors (GNSS-CLIMATCH [*Kirchengast et al.*, 2000; *Steiner et al.*, 2001; *Foelsche et al.*, 2003]) indicate the potential but also the weaknesses of state-of-the-art RO retrieval algorithms. The seasonal mean dry temperature bias (not including the sampling error) of an assumed RO monitoring system consisting of six LEO satellites would be below 0.2 K at most latitudes and altitudes between 8 and 30 km. Above 30 km the bias increases drastically, and in the high-latitude winter region an additional bias on the order of 1 K exists.

[7] Both the first GNSS-CLIMATCH and CHAMP results show the challenging areas of RO retrieval [see also *Kursinski et al.*, 1997; *Steiner et al.*, 2001; *Rieder and Kirchengast*, 2001]: the upper stratosphere, where the signal-to-noise ratio gradually becomes smaller as height increases toward the stratopause and into the mesosphere and thus where thermal noise, residual ionospheric error, and other small errors become increasingly important and the lower to middle troposphere where moisture and strong horizontal gradients complicate the interpretation of RO data. Currently, extensive research is ongoing on the latter topic [e.g., *Gorbunov*, 2002a, 2002b; *Jensen et al.*, 2003; *Ao et al.*, 2003; *Sokolovskiy*, 2003; *Beyerle et al.*, 2004], which is outside the scope of this work. This paper focuses on the former topic, the advancement of RO retrieval in the upper stratosphere, which is based on the evaluation of the performance of present state-of-the-art schemes.

[8] In section 2 the relevant methodology is described in detail. The results of the evaluation of present schemes and of the performance of a newly developed advanced scheme are discussed in section 3. Section 4, finally, provides a summary, the main conclusions, and an outlook.

## 2. Methodology

### 2.1. High-Altitude RO Retrieval Techniques

#### 2.1.1. RO Retrieval Overview

[9] The primary observables of RO measurements are the phase delays of GNSS signals (GPS: $\Phi_1, f_1$ = 1575.42 MHz;

$\Phi_2$, $f_2$ = 1227.60 MHz), i.e., the consequences of deceleration of the electromagnetic wave's phase velocity by the atmosphere. Doppler shifts and subsequently total bending angles $\alpha$ of the rays are deduced from phase delays. The refractive index $n$ can then be derived via the inverse Abel transform [*Fjeldbo et al.*, 1971],

$$n(a) = \exp\left[\frac{1}{\pi}\int_a^\infty \frac{\alpha(a')}{\sqrt{a'^2 - a^2}}da'\right], \quad (1)$$

from which the refractivity as a function of height, $N(z)$, is obtained via $N(a) = 10^6(n(a) - 1)$ and $z(a) = a/n(a) - R_C$. $R_C$ is the radius of curvature of the ellipsoidal Earth at the occultation location along the occultation plane (approximately Earth's radius), and $a$ is the ray's impact parameter (see Figure 1). Refractivity is related to total atmospheric pressure $p$, temperature, $T$, and the partial pressure of water vapor, $p_w$, via

$$N = k_1\frac{p}{T} + k_2\frac{p_w}{T^2}, \quad (2)$$

where $k_1$ and $k_2$ are constants ($k_1$ = 77.60 K hPa$^{-1}$, $k_2$ = 3.73 $\times$ 10$^5$ K$^2$ hPa$^{-1}$ [e.g., *Bevis et al.*, 1994]).

[10] Using the refractivity equation (2), the hydrostatic equation, the equation of state, and the gravity formula, the atmospheric parameters can be derived. For example, dry pressure $p_d(z)$ (which equals the total air pressure $p(z)$ if humidity can be neglected, i.e., above the middle troposphere) is obtained via hydrostatic integration:

$$p_d(z) = \frac{M_d}{k_1 R}\int_z^\infty g(z')N(z')dz', \quad (3)$$

where $R$ is the universal gas constant (8.3145 $\times$ 10$^3$ J K$^{-1}$ kg$^{-1}$), $M_d$ is the molar mass of dry air (28.964 kg kmol$^{-1}$), and $g(z)$ is the acceleration of gravity. Dry temperature is then $T_d(z) = k_1\, p_d(z)/N(z)$.

[11] For the retrieval of temperature and humidity in the lower and middle troposphere, a priori information on at least one of the two parameters is necessary. A detailed treatment of RO retrieval techniques is given by the *Kursinski et al.* [1997] review.

[12] The integration formulae, equations (1) and (3), are crucial links in the RO retrieval chain. Equation (1) indicates that the inversion of bending angles leads to downward propagation of high-altitude bending angle errors. Because of the localized kernel $(a'^2 - a^2)^{-1/2}$ of the inverse Abel transform, the vertical correlation of errors is still limited in $N(z)$, but further error propagation occurs via the hydrostatic integration, equation (3). It is thus vital to use adequate bending angles also at altitudes above any height of interest. A detailed discussion of RO retrieval error propagation in dry air is provided by *Rieder and Kirchengast* [2001].

### 2.1.2. Ionospheric Correction

[13] Ionospheric effects dominate the RO bending angles at heights above ~45 km [e.g., *Hocke*, 1997]. Since the ionosphere, as a dispersive medium, leads to different phase delays $\Phi_1$ and $\Phi_2$, and subsequently bending angles $\alpha_1$ and $\alpha_2$, these effects can be removed to first order by linear combination of the two signals. The traditional approach to do so is the linear correction of phase delays [e.g., *Spilker*, 1980],

$$\Phi_{LC}(t) = \frac{f_1^2\Phi_1(t) - f_2^2\Phi_2(t)}{f_1^2 - f_2^2}, \quad (4)$$

where $\Phi_{LC}$ is corrected phase delay and $t$ is the time.

[14] In recent applications the method of linear correction of bending angles has been applied more successfully [*Vorob'ev and Krasil'nikova*, 1994]:

$$\alpha_{LC}(a) = \frac{f_1^2\alpha_1(a) - f_2^2\alpha_2(a)}{f_1^2 - f_2^2}, \quad (5)$$

where $\alpha_{LC}$ is the corrected bending angle, and $\alpha_1$ and $\alpha_2$ are the uncorrected bending angles of the two signals at impact parameter $a$. As shown in several theoretical and simulation studies, the linear correction of bending angles provides better results, since it accounts for different ray paths of the two signals and exploits the fact that most of the total bending angle is accumulated near the ray perigee [e.g., *Vorob'ev and Krasil'nikova*, 1994; *Ladreiter and Kirchengast*, 1996].

[15] There are some methods that account for higher-order effects of the ionosphere [e.g., *Gorbunov et al.*, 1996a; *Syndergaard*, 2000], but these rely on additional a priori knowledge and on the assumption of spherical symmetry in the ionosphere. In section 2.2 we present a high-altitude RO retrieval evaluation study that, among other matters, systematically tested the ionospheric correction of bending angles under different large-scale ionospheric asymmetry conditions and different ionization levels. Effects of ionospheric small-scale variations (''ionospheric scintillations''), which act to increase random noise on top of receiver thermal noise and clock noise and which are amplified by the linear signal combination [e.g., *Kursinski et al.*, 1997], are not dealt with in this study; these need careful filtering in the processing of real data [e.g., *Gorbunov*, 2002c, and references therein].

### 2.1.3. Review of High-Altitude Initialization/Statistical Optimization Methods

[16] Even after ionospheric correction, retrieval results at heights above 20–30 km are sensitive to residual ionospheric noise (higher-order terms) and other noise (e.g., receiver thermal noise). This calls for sensible use of RO data at high altitudes, i.e., in the stratopause region and above. Additionally, since its upper integration limit ranges to infinity, the inverse Able transform needs some kind of high-altitude initialization of the bending angle profile in any case. The simplest way to do so is to select an upper boundary height (UBH) at altitudes between 50 and 70 km above which an extrapolated exponential profile is used [e.g., *Kursinski et al.*, 1997]. This approach (''exponential extrapolation'' or ''no optimization'' hereinafter) features several weaknesses, the most important ones being the sensitivity of retrievals to the exact UBH setting and to extrapolation quality due to measurement noise as well as the intrinsic assumption of an isothermal (constant scale height) atmosphere above the UBH. The latter assumption leads to a systematic bias in any ensemble of retrieved

profiles, which unfavorably is also UBH-dependent, since isothermality above 50–70 km insensibly ignores the actual mesosphere/lower thermosphere temperature structure.

[17] A more robust and sensible approach is statistical optimization, a form of optimal estimation [*Turchin and Nozik*, 1969; *Rodgers*, 2000]. It finds the most probable bending angle profile $\alpha_{\mathrm{opt}}$ by combining the observed profile with a background profile in a statistically optimal way [*Sokolovskiy and Hunt*, 1996; *Rodgers*, 2000]. The general effect of statistical optimization is that at higher altitudes, where the observation error exceeds the error of the background, the background determines $\alpha_{\mathrm{opt}}$. At lower altitudes, where the background error becomes dominant, the observed data determine $\alpha_{\mathrm{opt}}$. The transition zone between these two regimes lies typically between 45 and 60 km, depending on the error characteristics of the observed and background data. Note that statistical optimization does not improve the quality of observed profiles themselves at high altitudes but rather delivers an improved combined profile thanks to the sensible inclusion of background information. The most important effect is that downward propagation of errors via the inverse Abel transform and the hydrostatic integral is reduced.

[18] Background profiles can be obtained from climatological models or profile data sets or from NWP analyses or forecasts. Since the quality of NWP analyses at high altitudes (above ~30 km) is still poor, because of the sparseness of adequate assimilated data at these heights, and since the RO-retrieved profiles may later be evaluated using these analyses or even be used in the data assimilation process producing them (which would result in "incest" problems), we presently prefer the use of climatological models like MSISE-90 [*Hedin*, 1991] or Committee on Space Research (COSPAR) International Reference Atmosphere (CIRA-86) [*Fleming et al.*, 1988]. Previous work cited in the paragraphs below also used either of these two standard climatologies, which are closely similar in the height range 30–120 km.

[19] The full optimization formula which optimally combines, in a least squares sense, observations and background reads ("inverse covariance weighting" optimization hereinafter) is as follows:

$$\alpha_{\mathrm{opt}} = \alpha_b + \mathbf{B}(\mathbf{B}+\mathbf{O})^{-1}(\alpha_o - \alpha_b), \tag{6}$$

where $\alpha_b$ and $\alpha_o$ are the background and observed bending angle profiles, and $\mathbf{B}$ and $\mathbf{O}$ are the background and observation error covariance matrices, respectively. The assumptions of this approach are that unbiased (Gaussian) errors and a linear problem are assumed. Linearity is fulfilled in the present case, and the unbiased error assumption holds reasonably well for the observation error due to the self-calibrating nature of RO measurements. The background errors are likely to involve biases in addition to their random component, however. Consequently, biases in background data, which could partially leak into retrievals and thereby degrade the climate monitoring utility of retrieved profiles, are an important problem in the practical application of statistical optimization and are thus one key matter of this paper.

[20] Since it is difficult to obtain accurate covariance matrices, *Sokolovskiy and Hunt* [1996] used a simpler form assuming vertically uncorrelated errors. This allows to calculate the optimized bending angles ray-per-ray ("inverse variance weighting" optimization hereinafter):

$$\alpha_{\mathrm{opti}} = \alpha_{bi} + \frac{\sigma_{bi}^2}{\sigma_{bi}^2 + \sigma_{oi}^2}(\alpha_{oi} - \alpha_{bi}), \tag{7}$$

where $i$ is a height index, and $\sigma_{bi}$ and $\sigma_{oi}$ are the estimated standard deviations of the background and the observation data, respectively. $\sigma_{bi}$ is typically assumed to be a constant fraction of the background bending angle profile (5–20%), and $\sigma_{oi}$ is estimated, generally as a constant $\sigma_o$, from the root-mean-square (RMS) error of the observed profile compared to the background or from the high-frequency variations of the observed signal, within a high-altitude range of 10–15 km above 65 km, where noise dominates the signal [*Gorbunov et al.*, 1996b; *Gorbunov and Gurvich*, 1998; *Hajj et al.*, 2002].

[21] A modification of this inverse variance weighting is the "heuristic weighting" optimization [*Hocke et al.*, 1997; *Hocke*, 1997; *Steiner et al.*, 1999],

$$\alpha_{\mathrm{opti}} = \alpha_{bi} + \frac{\sigma_{bi}}{\sigma_{bi} + \sigma_{oi}}(\alpha_{oi} - \alpha_{bi}), \tag{8}$$

where $\sigma_{bi}$ is again assumed to be a constant fraction of the background bending angle (typically 20%), but $\sigma_{oi}$ is defined to be the absolute difference between the observed profile and the background at each height $i$, $\sigma_{oi} = |\sigma_{oi} - \sigma_{bi}|$. This approach effectively weighs down "outliers" and smoothes the profile at high altitudes but is nonoptimal in a formal statistical sense and tends to produce retrievals biased toward the background [see also *Healy*, 2001].

[22] *Healy* [2001] suggested to use the full inverse covariance weighting approach, equation (6), and demonstrated it with a simplified analytical background error covariance matrix of Gaussian shape,

$$B_{ij} = \sigma_{bi}\sigma_{bj} \exp\left[-\frac{(a_i - a_j)^2}{L^2}\right], \tag{9}$$

where $B_{ij}$ are the elements of the error covariance matrix $\mathbf{B}$, $\sigma_{bi}$ and $\sigma_{bj}$ are background standard errors at heights $i$ and $j$, $a_i$ and $a_j$ are the impact parameters, and $L$ is the error correlation length. $L$ was set to 6 km and $\sigma_{bi}$ again to 20% of the background value. Regarding observation errors, a constant vertically uncorrelated error $\sigma_o$ set to 5 μrad was assumed.

[23] A somewhat similar (applying inverse covariance weighting as well) but more general concept was introduced and discussed by *Rieder and Kirchengast* [2001], who generalized the treatment of the optimization problem to employ the full breath of the optimal estimation methodology detailed by *Rodgers* [2000]. In demonstrating the concept, the background bending angle errors $\sigma_{bi}$ were set to linearly increase from 6 to 18% of the background profile between 30 and 120 km; the background covariances were analytically derived according to equation (9). Though the demonstration started with phase delay observations, the

concept can be equally well used starting with bending angles.

[24] *Gorbunov* [2002c] proposed a combined ionospheric correction and statistical optimization algorithm where the background is linearly fitted to the observations between 40 and 60 km to reduce the background bias, observation and background errors are assumed to be vertically uncorrelated, and both $\sigma_o$ and $\sigma_b$ are dynamically estimated: $\sigma_o$ is estimated from the variance of the observation above 50 km, and $\sigma_b$ is estimated from the RMS deviation between background and observations between 12 and 35 km.

[25] An alternative to the inversion approach described in section 2.1.1 is the assimilation of observed (ionosphere-corrected) bending angle profiles with forward modeled background data using one-dimensional (1-D) variational data assimilation as proposed and described, e.g., by *Eyre* [1994], *Palmer et al.* [2000], and *von Engeln et al.* [2003]. Using this approach, the observed data are only processed to the bending angle level, and no further inversion is applied. The main challenges using this approach are the adequate definition of the forward modeling operators and background error covariance matrices as well as the lack of a simple method to cope with biases in the background data.

### 2.1.4. Basic IGAM High-Altitude Retrieval Scheme

[26] The basic high-altitude retrieval scheme used at IGAM applies the linear correction of bending angles, equation (5), followed by inverse covariance weighting, equation (6), using MSISE-90 bending angle profiles as background together with an analytical background error covariance matrix with an error correlation length of $L$ = 6 km. Different from *Healy* [2001], exponential decay of covariances was used:

$$B_{ij} = \sigma_{bi}\sigma_{bj} \exp\left[-\frac{|a_i - a_j|}{L}\right], \tag{10}$$

which was found to be more adequate in an empirical error study by *Steiner and Kirchengast* [2004]. Observation errors $O_{ij}$ were specified in the same form as $B_{ij}$ but with a shorter correlation length ($L$ = 1 km) based as well on results by *Steiner and Kirchengast* [2004]. This short-range correlation accounts for the smoothing of the phase delays in an earlier step of the retrieval. The background standard deviation $\sigma_b$ is assumed to amount to 20% of the background bending angle, which is a frequently used estimate of the stratopause/mesosphere RMS uncertainty of the MSISE-90 climatology and is also based on retrieval performance studies conducted at IGAM (not presented here). The observation errors $\sigma_o$ are estimated from the RMS deviation of the observed bending angle profile compared to the background between 70 and 80 km, where the bending angle signal is at the $\leq$1 μrad level and ionospheric residual and measurement noise dominate. The optimization, equation (6), is applied from 120 km down to 30 km height, below which the signal-to-noise ratio is so strong that it is safely no longer required [e.g., *Rieder and Kirchengast*, 2001].

[27] S. Syndergaard (Institute of Atmospheric Physics, University of Arizona, personal communication, 1999) suggested to perform background search prior to statistical optimization, i.e., to fit the available ensemble of background profiles to the observed profile and use the best fit, instead of the colocated profile, as background in the statistical optimization process. We adopted this approach in the IGAM retrieval scheme, searching the global MSISE-90 climatology on a 5° latitude × 15° longitude grid through all months from January to December and using a least squares fit in the 45–65 km height interval to determine the best fit profile. Besides this statistical optimization of bending angles, no further background information is used in the IGAM scheme, different from most other retrieval chains, which also initialize the hydrostatic integral, equation (3), using data from NWP analyses or climatologies.

[28] The scheme, which was tested in a systematic high-altitude retrieval evaluation study [*Gobiet and Kirchengast*, 2002] and applied in the GNSS-CLIMATCH study (see section 1), already proved to be effective. However, it cannot cope with a situation where no unbiased data are available in the background climatology. As will be shown in section 3, for the MSISE-90 climatology this situation frequently occurs in the high-latitude winter region. Similar results were found by *Randel et al.* [2003] for the CIRA-86 climatology, which provided the basis for the MSISE-90 climatology below the thermosphere.

### 2.1.5. Enhanced IGAM High-Altitude Retrieval Scheme

[29] Considering the results from CHAMP, the GNSS-CLIMATCH study, and high-altitude retrieval evaluation studies presented in section 3, the most promising pathway to advance high-altitude RO retrieval is to pay more attention to biases in the background information used in the statistical optimization approach. Since, presently, no better mesospheric climatology than MSISE-90 (or CIRA-86) is available, and since direct use of NWP analyses as background is not desirable (see section 2.1.3), an extension to the background bias correction ability of the basic IGAM scheme was developed.

[30] The main components of the enhanced algorithm are linear ionospheric correction of bending angles, equation (5), empirical background bias correction of bending angles (explanation below), and inverse covariance weighting statistical optimization of bending angles, equation (6). These main components involve the following ingredients:

[31] 1. Background information consists of bending angle profiles derived from the MSISE-90 climatology. (Alternatively, the use of more diverse libraries of upper stratosphere/mesosphere bending angle profiles is studied, e.g., based on middle atmosphere Light Detection and Ranging (LIDAR) profile or Envisat/MIPAS limb sounder profile databases; also, ECMWF analyses may be useful, which currently do not reach beyond ~60 km, however.)

[32] 2. Empirical background bias correction, step 1, is as follows: Search the best fit bending angle profile in the climatology using a least squares criteria in the 45–65 km interval (section 2.1.4). The optimal height interval depends on the noise level of the observations. For testing this scheme we used the GRAS error specifications [e.g., *Global Navigation Satellite System Receiver for Atmospheric Sounding Science Advisory Group* (*GRAS-SAG*), 1998]. For more noisy observations (e.g., GPS/MET, CHAMP) it is necessary to place the fit interval at lower altitudes.

[33] 3. Empirical background bias correction, step 2, includes the following: adjustment of the background profile by multiplying it with a fitting coefficient (a factor usually close to unity) derived from regression with respect to the observed profile at high altitudes (least squares adjustment). A similar approach was suggested by *Gorbunov* [2002c], though that approach uses lower altitudes and was not combined with background search. Tests showed that the 55–75 km interval is especially sensitive for detecting remaining background biases. The optimal height interval depends on the observation noise level and the error characteristics of the background. Regarding the resulting optimized profile, it represents the region just above the transition zone from background dominated to observation dominated. GRAS error specifications were used when testing the correction. For more noisy observations (e.g., GPS/MET, CHAMP) it is necessary to use a lower altitude range.

[34] 4. Standard deviation of background error is set to 15% (instead of 20%) of the background bending angle profile (accounting for the bias reduction and determined in empirical tests), vertically correlated over about a scale height.

[35] 5. Standard deviation of observation error is estimated from the RMS deviation of the observed bending angle profile compared to the background (after bias correction) within 70–80 km, weekly vertically correlated; see equation (10).

[36] The key advancement of this scheme is its bias correction before the optimization, which is done in an empirical way by comparing the background to the observations within suitable altitude ranges. It combines the advantages of the near bias-free observations and the small statistical error of the background. Step 1 means that the climatology is used as a library of representative bending angle profiles and the best fit profile is chosen as background. Step 2 means that if there is no well-fitting profile in the library, there is the possibility to adjust the background profile toward the observed profile.

### 2.2. High-Altitude RO Retrieval Evaluation Studies

[37] The performance of the high-altitude RO retrieval schemes was evaluated in a twofold way: The first part was a systematic case study, which focused on individual occultation events and their error characteristics under different ionospheric conditions. The second part was a large-sample study focusing on sample error statistics and spatial (latitudinal) distribution of errors. Both parts were based on end-to-end simulations of RO events, which provides the advantage that the "true" state of the atmosphere is known and a detailed error analysis is possible. The complete study, beginning with satellite geometry simulation and proceeding with modeling of GNSS signal propagation through the atmosphere/ionosphere, simulation of the observation system and the observables, and retrieval of the atmospheric profiles, was performed by means of a study-tailored version of the End-to-end GNSS Occultation Performance Simulator (EGOPS) software tool [*Kirchengast et al.*, 2002].

#### 2.2.1. Systematic Case Study Setup

[38] The setup of this study is described in some detail by *Gobiet and Kirchengast* [2002]. In the framework of this paper we expanded it by two additional retrieval schemes.

[39] In order to study the effects of statistical optimization as a function of ionospheric state, we choose three occultation events (out of a sample consisting of ~2100 events) as base scenarios, each of them being representative for one type of symmetry or asymmetry of electron density distribution in the ionosphere. For the sake of brevity we refer to them as the "Nice," "Nasty 1," and "Nasty 2" events hereinafter. We simulated the propagation of radio signals through the atmosphere without ionosphere ("no ionosphere" reference case) as well as at three different ionization levels, represented by the radio flux at 10.7 cm ($F_{10.7}$ index) ranging from $F_{10.7} = 70$ through $F_{10.7} = 140$ to $F_{10.7} = 210$ (low, middle, and high solar activity).

[40] The ionosphere model utilized in the simulation was the Electron Density, University of Graz (NeUoG) model [*Leitinger and Kirchengast*, 1997a]. NeUoG provides global 3-D electron density distributions depending on local time, season, and solar activity. It features reasonably realistic climatological ionization conditions and has already proven to be useful in the past in occultation-related studies [e.g., *Leitinger and Kirchengast*, 1997b] but does not feature small-scale structures. This latter restriction should be kept in mind when interpreting the results of this study.

[41] The Nice event (Figure 2a) was chosen to be zonally oriented. By this, and because of careful selection of the occultation event location, the spherical symmetry assumption is met as good as is possible in a realistic ionosphere during daytime conditions. The two Nasty events (Figures 2b and 2c) were chosen to be meridionally oriented and probe through severe electron density gradients associated with the equatorial anomaly, each violating the spherical symmetry assumption in a specific distinct manner. The Nasty 1 event exhibits relatively low electron densities at the in and out bounds of the occultation rays and a maximum in electron density above the occultation tangent point. The Nasty 2 event exhibits low electron densities at the in bound and high electron densities at the out bound of the occultation rays.

[42] Since the aim of the study is to describe the effects of the ionospheric conditions and the method of high-altitude initialization on the RO retrieval products rather than effects of error sources internal to the neutral atmosphere, we supplied the forward model with a simple neutral atmosphere in order to ensure that the errors in the subsequently retrieved atmospheric parameters would be fully traceable to ionospheric residuals and the method of statistical optimization. We used a dry atmosphere, local spherical symmetry, and identical conditions for all three simulated occultation events. The neutral atmosphere employed this way was one selected vertical profile out of the MSISE-90 climatology, i.e., the same climatology we used as background in the statistical optimization process. This adds some interesting aspects to the interpretation of the results (section 3.1). We chose the profile colocated with the Nice event (63°N, 93°E; month September).

[43] Additionally, two different receiving systems were modeled: an idealized, where observation system–related errors were neglected, and a "realistic" one, which was based on the error specifications of the GRAS receiver [e.g., *GRAS-SAG*, 1998] and included the main receiving system related errors such as orbit uncertainties, receiver noise,

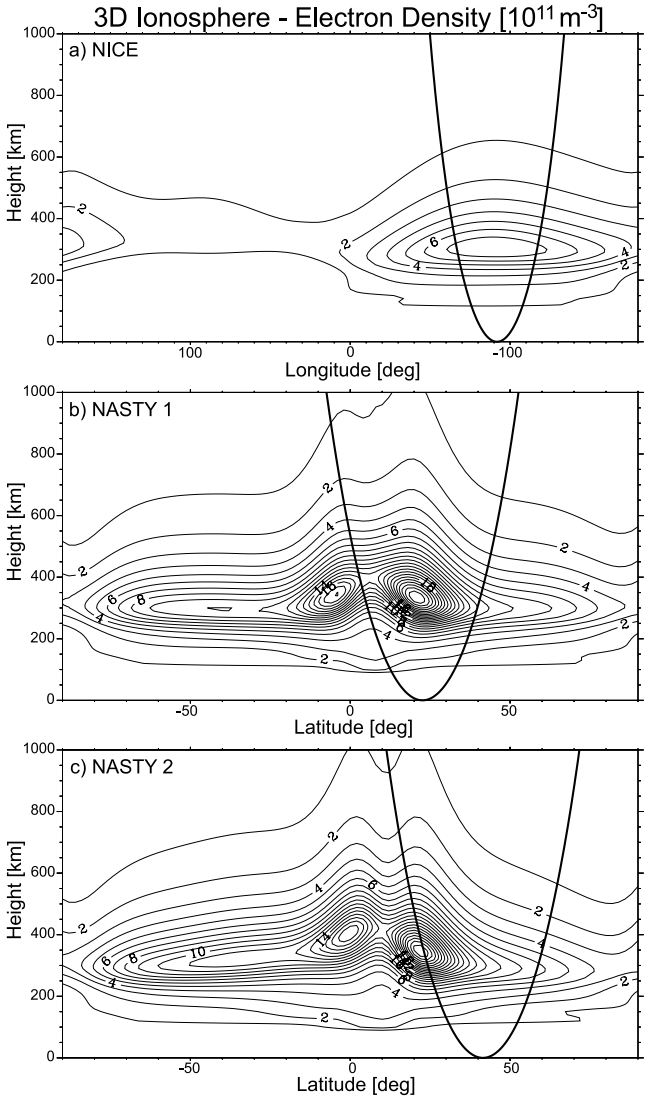


**Figure 2.** Ionospheric conditions for the three representative occultation events (for $F_{10.7}$ = 140). (a) "Nice" event. Vertical total electron content (TEC) above tangent point is $\sim 20 \times 10^{16}$ m$^{-2}$; electron density varies $<1.5 \times 10^{11}$ m$^{-3}$ between inbound and outbound of lowermost ray. (b) "Nasty 1" event. Vertical TEC above tangent point is $\sim 60 \times 10^{16}$ m$^{-2}$; electron density varies $\sim 12 \times 10^{11}$ m$^{-3}$ between inbound and outbound of lowermost ray and is maximal above tangent point. (c) "Nasty 2" event. Vertical TEC above tangent point is $\sim 25 \times 10^{16}$ m$^{-2}$; electron density varies $\sim 18 \times 10^{11}$ m$^{-3}$ between inbound and outbound of lowermost ray and is maximal at outbound.

local multipath errors, and clock errors. Subsequently, we performed the retrieval using five different retrieval scheme settings.

[44] We show results for no optimization (with observed profile exponentially extrapolated; section 2.1.3), heuristic weighting optimization, equation (8), inverse covariance weighting optimization without (basic IGAM without search) and with (basic IGAM with search) background search (section 2.1.4), and inverse covariance weighting with enhanced background bias correction (enhanced IGAM; section 2.1.5). In total, 24 different scenarios were modeled (three representative events times four ionization levels times two receiving system types), and each of these 24 scenarios was evaluated using the five different retrieval schemes. Results of this study are discussed in section 3.1.

#### 2.2.2. Large Ensemble Study Setup

[45] Selected RO retrieval schemes were also tested using a large ensemble of quasi-realistically simulated occultation events. For allowing comparison to earlier results, we used a simulated occultation event ensemble, which is globally distributed and was originally produced in the framework of the GNSS-CLIMATCH study (section 1). It involves the simulation of a six-satellite constellation, each satellite equipped with a GRAS-type receiver. The neutral atmosphere modeling used a middle atmosphere–extended version of the European Center/Hamburg (ECHAM4) general circulation model (GCM) [*Roeckner et al.*, 1999] with a horizontal resolution of $\sim 2.8°$ and 39 vertical levels up to 0.01 hPa or $\sim$80 km (T42L39 resolution). Above $\sim$80 km the neutral atmosphere was extrapolated using the MSISE-90 climatology. While typical current GCM fields, including ECMWF analyses, do not reach beyond 0.1 hPa, the GCM fields used here extend up to near the mesopause, which is important for the present assessment of retrieval schemes as it ensures that any search and best fit estimates are performed at height ranges governed by the more variable GCM conditions rather than the climatological conditions. The ionosphere was modeled using the NeUoG model. For more details see *Foelsche et al.* [2003, and references therein].

[46] The ensemble consists of $\sim$1000 occultation events that characterize the northern summer/southern winter season 1997 (June, July, and August) and are evenly distributed in time and space. For the analysis of error statistics and the latitudinal dependency of errors it was partitioned into 17 equal-area latitude bins of 10° width (equatorial bin is 10° latitude × 15° longitude), each containing 50–60 occultation events [*Foelsche et al.*, 2003]. We used this ensemble to systematically test the performance of three different high-altitude retrieval schemes (no optimization, basic IGAM with search, and enhanced IGAM; see section 2.2.1), with focus on the latitude-height distribution of biases. Results of this study are discussed in section 3.2.

## 3. Results and Discussion

### 3.1. Systematic Case Study

[47] Figure 3 gives an overview on the performance of the no optimization retrieval and the inverse covariance weighting optimization retrieval with search in MSISE-90 applied to the 24 simulated scenarios. Each bar in Figure 3 represents the mean temperature error between 35 and 45 km ("upper stratosphere bias" hereinafter) of one specific scenario. At these altitudes the RO-retrieved temperatures are heavily influenced by background information, thus the upper stratosphere bias indicates the bias in the background or in the exponentially extrapolated bending angle profile, respectively.

[48] The most salient result is the strong mitigation of the upper stratosphere bias by statistical optimization. Without optimization the behavior of the retrieval above $\sim$30 km depends heavily on noise in the data. One and the same

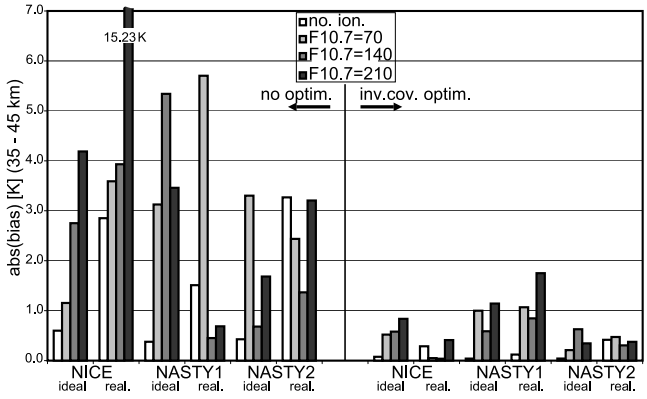


**Figure 3.** Mean error of the retrieved temperature between 35 and 45 km (“upper stratosphere bias”) for all simulated occultation scenarios (three events, four ionization levels, ideal and realistic receiving system). (left) No optimization (no optim.) retrieval. (right) Basic IGAM retrieval with search for best fit background (inv. cov. optim.).

simulated occultation event can give different upper stratosphere biases of up to 20 K, depending on the starting value of the random number generator used in the simulation of receiver noise. Applying statistical optimization (in this case the basic IGAM scheme) strongly stabilizes the retrieval, makes it robust against random noise and residual ionospheric errors and retains the upper stratosphere bias below 1 K in most cases. Additionally, it is shown for the linear ionospheric correction of bending angles that neither highly asymmetric ionospheric conditions nor high ionization levels do significantly degrade the retrieval performance, especially when statistical optimization is applied, as one should expect as long as noise due to small-scale ionospheric structures is small [e.g., *Gorbunov*, 2002c, and references therein]. Figure 4 shows the error profiles of temperature for one example occultation scenario (Nasty 1, $F_{10.7} = 70$, realistic receiving system) retrieved with the five different high-altitude retrieval schemes introduced in section 2.2.1.

[49] In this scenario the colocated background profile from MSISE-90 is biased, since we used a different neutral atmosphere profile (from the Nice event) in the forward modeling (see section 2.2.1). However, inspection shows that the background error is <8% in the stratosphere and mesosphere, which is clearly within the assumed uncertainty of 20%. The example scenario can thus be considered representative for a real RO retrieval situation.

[50] Figure 4a shows that errors due to deficient high-altitude initialization can propagate down to below 20 km in the temperature profile. While this may be considered a “bad case,” error propagation down to <30 km will be common. Heuristic weighting optimization (Figure 4b) stabilizes the retrieval, but it is strongly biased toward the background. The inverse covariance weighting optimization without search leads to much better results (Figure 4c), but the temperature stays biased toward the background. The retrieval with search (Figure 4d) is able to account for the biased background and manages to find an unbiased background profile. The retrieval results stay virtually unbiased up to 40 km. This demonstrates the situation, when a search library is adequate, i.e., when an unbiased profile is available in the library. In such a situation a second step of background bias reduction is not necessary, and the enhanced IGAM retrieval (Figure 4e) gives essentially the same result as the basic IGAM with search retrieval. In the example shown here (Figure 4e), the enhanced IGAM retrieval is still slightly better than the basic one with search, while in other cases it can also be slightly worse or closely the same but never far away from the basic retrieval (difference of upper stratosphere bias <0.5 K), as one expects for an adequate search library.

### 3.2. Large Ensemble Study

[51] The ECHAM4 model was used to create neutral atmospheric fields representing the summer season 1997 for the simulation of a large ensemble of occultation events (∼1000 events; see section 2.2.2). Contrary to the systematic

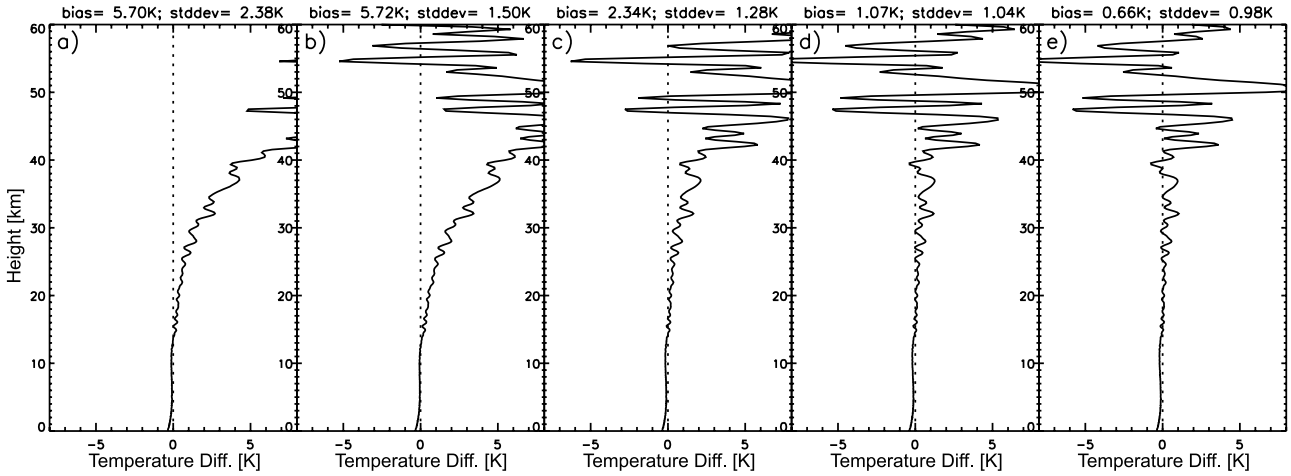


**Figure 4.** Temperature error profiles for the Nasty 1 occultation event (asymmetric conditions, $F_{10.7} = 70$, realistic receiver) retrieved with different high-altitude retrieval schemes: (a) no optimization, (b) heuristic weighting optimization, (c) basic IGAM without search, (d) basic IGAM with search, and (e) enhanced IGAM. Standard deviation (stddev) is also listed.

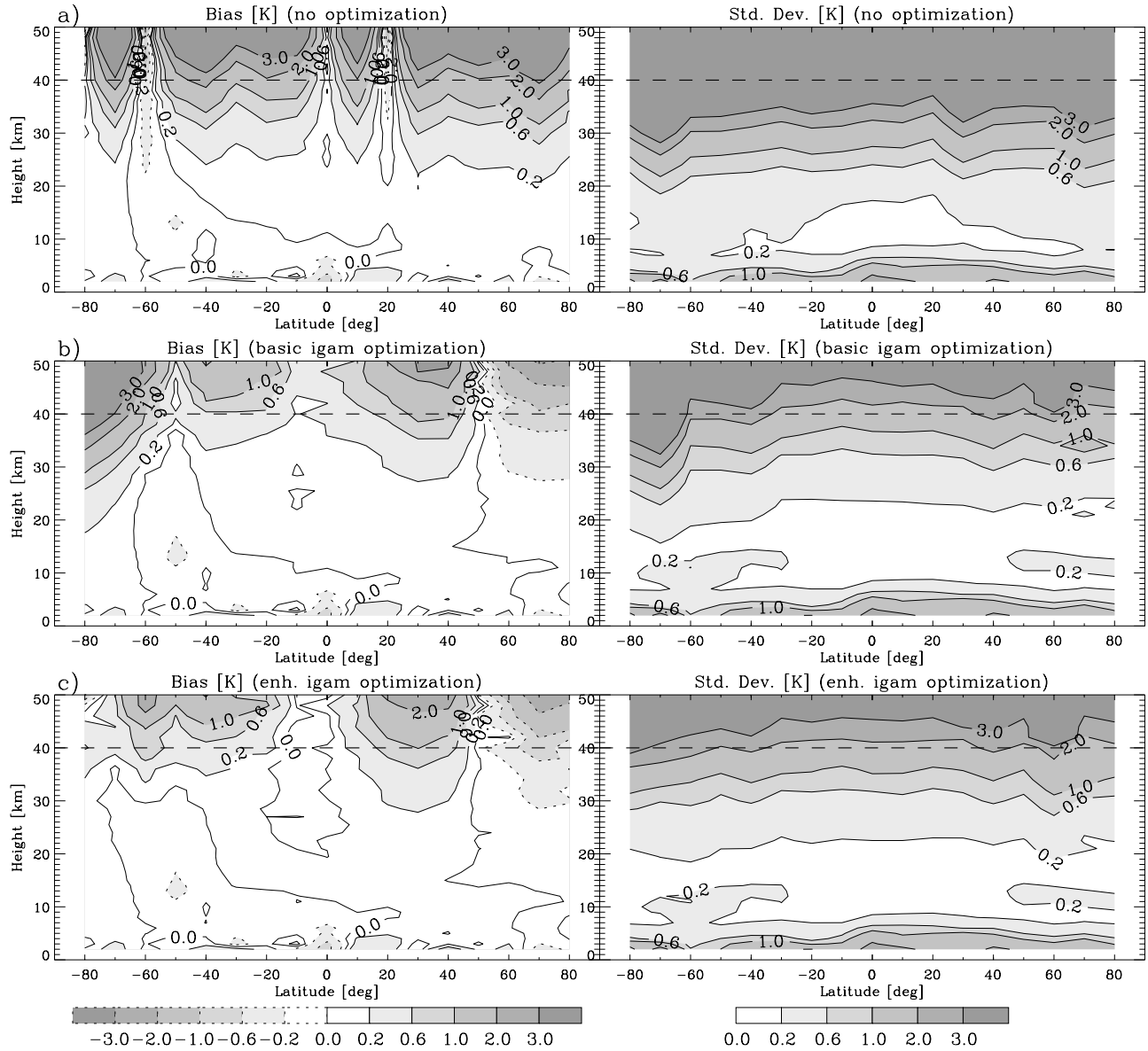


**Figure 5.** (left) Seasonal mean bias and (right) standard deviation of temperature retrieved from an ensemble of ~1000 simulated occultation events. High-altitude retrieval schemes are as follows: (a) no optimization, (b) basic IGAM with search, and (c) enhanced (enh.) IGAM.

case study, this setup does not automatically ensure that an unbiased background profile is available for each retrieval, since the forward model atmosphere is different from the MSISE-90 climatology used for background information. The MSISE-90 search library may thus be partially inadequate, which is a situation more realistic but also more demanding for the statistical optimization scheme. Figure 5 shows latitude versus height slices of the dry temperature retrieval seasonal mean bias and standard deviation for the no optimization, basic IGAM with search, and enhanced IGAM retrieval schemes.

[52] The no optimization case shows again that the high-altitude retrieval performance is very unstable if the bending angle profile is simply exponentially extrapolated. The >1 K standard deviation region starts at ~25 km, which is ~10 km lower than in the two optimization cases. The most salient improvement of the enhanced IGAM algorithm over the basic IGAM with search algorithm is the drastic error reduction in the southern high-latitude region, where the MSISE-90 search library is most inadequate. Less salient, but robustly evident, is furthermore a general improvement of the retrieval quality above 30 km.

[53] The additional bias correction step of the enhanced IGAM scheme exhibits the behavior of an "emergency reserve": In most cases, where the background library is adequate, the background bending angles are only slightly modified (~1%), and the effect on the retrieved temperatures below 40 km is small. In the cases, however, when no unbiased background profile is found in the library, the modification reaches up to 15%, and significant improvement is achieved. For these cases the MSISE-90 climatology is inadequate to supply profiles unbiased against the

ECHAM4 model atmosphere used. The capability of the enhanced IGAM scheme to handle these conditions is important since also in cases of real data, existing climatological libraries will not be able to supply adequate background profiles under all conditions.

## 4. Summary, Conclusions, and Outlook

[54] An enhanced statistical optimization scheme for GNSS RO retrievals was presented. This and other retrieval schemes were tested in two retrieval performance studies, one based on representative profile scenarios, the other on a large ensemble of profiles.

[55] Sensible statistical optimization of bending angles is found vital to obtain results of good quality in the upper stratosphere. In this context it is shown for the linear ionospheric correction of bending angles that neither highly asymmetric ionospheric conditions nor high ionization levels do significantly degrade the retrieval performance, as one should expect as long as noise due to small-scale ionospheric structures (ionospheric scintillations) is small. The latter has been disregarded in this investigation; in the processing of real data, it needs separate care in filtering before correction.

[56] Using statistical optimization, it is found that the retrieval performance can be significantly improved further if biases in the background information are corrected. Since the statistical optimization method fundamentally assumes unbiased errors, potential biases need to be removed before the optimization. The ''enhanced IGAM scheme'' presented incorporates a two-step empirical background bias correction: A first step searches and extracts a best fit profile (fitting over the stratopause height range) from a suitable library of profiles instead of using the colocated profile, and a second step adjusts this best fit profile toward the observed profile (by fit over the lower mesosphere height range), further compensating potential bias in the best fit profile if existing. The exact height ranges for fitting depend on the observational noise in the RO data; the higher the noise the lower down these height ranges (the present study used the European GRAS receiver as baseline). The bias correction is particularly effective when background data are systematically inadequate, as was found in this work in the high-latitude winter atmosphere.

[57] Use of an independent search library for best fit selection of background profiles (e.g., the MSISE-90 climatology) rather than colocated NWP analysis profiles (e.g., from ECMWF) avoids introducing potential analysis biases into RO climatologies. Moreover, validation of RO retrievals relative to analysis fields needs independency of the RO data from these reference data. Improved search libraries than the currently available MSISE-90 and CIRA-86 climatologies should be built in the future (e.g., from middle atmosphere LIDAR data or Envisat/MIPAS data) in order to ensure that adequate background profiles are available for all the diverse stratosphere and mesosphere conditions of different locations and seasons.

[58] Follow-on work focuses on evaluation of the IGAM retrieval schemes by applying them to RO data from the CHAMP mission and employing them in validation studies using correlative data from MIPAS and GOMOS on Envisat, radiosondes, and ECMWF analyses. Via this evaluation we aim at further algorithm improvements especially related to different observation noise levels and to quality control. For the lower to middle troposphere a complementary advanced wave optics retrieval algorithm will be employed. The retrieval algorithm package will then be used at large scale to create RO-based global climatologies of refractivity, geopotential height, temperature, and humidity, starting with RO data from CHAMP and SAC-C. Later, data from next missions such as GRACE, GRAS on MetOp, and COSMIC will be used as well.

[59] **Acknowledgments.** The authors thank U. Foelsche and A. K. Steiner for valuable support concerning the link to the GNSS-CLIMATCH study and for fruitful scientific discussions. M. E. Gorbunov, S. B. Healy, and S. Syndergaard are thanked for providing important stimuli for some parts of the work. J. Fritzer and J. Ramsauer provided helpful assistance regarding modification and use of the EGOPS software. A.G. received financial support for the work from the START research award of G.K. funded by the Austrian Ministry for Education, Science, and Culture and managed under program Y103-N03 of the Austrian Science Fund.

## References

Anthes, R. A., C. Rocken, and Y. Kuo (2000), Applications of COSMIC to meteorology and climate, *Terr. Atmos. Oceanic Sci.*, *11*(1), 115–156.

Ao, C. O., T. K. Meehan, G. A. Hajj, A. J. Mannucci, and G. Beyerle (2003), Lower troposphere refractivity bias in GPS occultation retrievals, *J. Geophys. Res.*, *108*(D18), 4577, doi:10.1029/2002JD003216.

Bevis, M., S. Businger, T. A. Herring, C. Rocken, R. A. Anthes, and R. H. Ware (1994), GPS meteorology: Mapping zenith wet delays onto precipitable water, *J. Appl. Meteorol.*, *33*, 379–386.

Beyerle, G., J. Wickert, T. Schmidt, and C. Reigber (2004), Atmospheric sounding by GNSS radio occultation: An analysis of the negative refractivity bias using CHAMP observations, *J. Geophys. Res.*, *109*, D01106, doi:10.1029/2003JD003922.

Edwards, P. G., and D. Pawlak (2000), MetOp: The space segment for EUMETSAT's polar system, *ESA Bull.*, *102*, 6–18.

Eyre, J. R. (1994), Assimilation of radio occultation measurements into a numerical weather prediction system, *Tech. Memo. 199*, Eur. Cent. Medium-Range Weather Forecasts Res. Dep., Reading, U. K.

Fishbach, F. F. (1965), A satellite method for temperature and pressure below 24 km, *Bull. Am. Meteorol. Soc.*, *9*, 528–532.

Fjeldbo, G. F., V. R. Eshleman, and A. J. Kliore (1971), The neutral atmosphere of Venus as studied with the Mariner V radio occultation experiments, *Astron. J.*, *76*, 123–140.

Fleming, E. L., S. Chandra, M. R. Shoeberl, and J. J. Barnett (1988), Monthly mean global climatology of temperature, wind, geopotential height and pressure for 0–120 km, *NASA Tech. Memo., TM-100697*, 85 pp.

Foelsche, U. (1999), Tropospheric water vapor imaging by combination of spaceborne and ground-based GNSS sounding data, Ph.D. thesis, Inst. for Geophys., Astrophys., and Meteorol., Univ. of Graz, Graz, Austria.

Foelsche, U., G. Kirchengast, and A. K. Steiner (2003), Global climate monitoring based on CHAMP/GPS radio occultation data, in *Proceedings of 1st CHAMP Science Meeting*, pp. 397–407, Springer, New York.

Global Navigation Satellite System Receiver for Atmospheric Sounding Science Advisory Group (GRAS-SAG) (1998), The GRAS instrument on MetOp, *ESA VR/3021/PI, EUMETSAT EPS/MIS/IN/9*, Eur. Space Agency/Eur. Space Res. and Technol. Cent., Noordwijk, Netherlands.

Gobiet, A., and G. Kirchengast (2002), Sensitivity of atmospheric profiles retrieved from GNSS occultation data to ionospheric residual and high-altitude initialization errors, *Tech. Rep. ESA/ESTEC-1/2002*, Inst. for Geophys., Astrophys., and Meteorol., Univ. of Graz, Graz, Austria.

Gorbunov, M. E. (2002a), Canonical transform method for processing radio occultation data in the lower troposphere, *Radio Sci.*, *37*(5), 1076, doi:10.1029/2000RS002592.

Gorbunov, M. E. (2002b), Radio-holographic analysis of Microlab-1 radio occultation data in the lower troposphere, *J. Geophys. Res.*, *107*(D12), 4156, doi:10.1029/2001JD000889.

Gorbunov, M. E. (2002c), Ionospheric correction and statistical optimization of radio occultation data, *Radio Sci.*, *37*(5), 1084, doi:10.1029/2000RS002370.

Gorbunov, M. E., and A. S. Gurvich (1998), Algorithms of inversion of Microlab-1 satellite data including the effects of multipath propagation, *Int. J. Remote Sens.*, *19*, 2283–2300.

Gorbunov, M. E., S. V. Sokolovskiy, and L. Bengtsson (1996a), Space refractive tomography of the atmosphere: Modeling of direct and inverse

problems, *Tech. Rep. 210*, Max Planck Inst. for Meteorol., Hamburg, Germany.

Gorbunov, M. E., S. V. Sokolovskiy, and L. Bengtsson (1996b), Advanced algorithms of inversion of GPS/MET satellite data and their application to reconstruction of temperature and humidity, *Tech. Rep. 211*, Max Planck Inst. for Meteorol., Hamburg, Germany.

Gurvich, A. S., and T. G. Krasil'nikova (1987), Navigation satellites for radio sensing of the Earth's atmosphere (in Russian), *Sov. J. Remote Sens.*, *6*, 89–93.

Hajj, G. A., E. R. Kursinski, L. J. Romans, W. I. Bertiger, and S. S. Leroy (2002), A technical description of atmospheric sounding by GPS occultation, *J. Atmos. Sol. Terr. Phys.*, *64*, 451–469.

Healy, S. B. (2001), Smoothing radio occultation bending angles above 40 km, *Ann. Geophys.*, *19*, 459–468.

Hedin, A. E. (1991), Extension of the MSIS thermosphere model into the middle and lower atmosphere, *J. Geophys. Res.*, *96*(A2), 1159–1172.

Hocke, H., G. Kirchengast, and A. Steiner (1997), Ionospheric correction and inversion of GNSS occultation data: Problems and solutions, *Tech. Rep. ESA/ESTEC 2/97*, Inst. of Meteorol. and Geophys., Univ. of Graz, Graz, Austria.

Hocke, K. (1997), Inversion of GPS meteorology data, *Ann. Geophys.*, *15*, 443–450.

Intergovernmental Panel on Climate Change (2001), *Climate Change 2001: The Scientific Basis: Contribution of Working Group I to the Third Assessment Report of the Intergovernmental Panel on Climate Change*, edited by J. T. Houghton et al., Cambridge Univ. Press, New York.

Jensen, A. S., M. S. Lohmann, H.-H. Benzon, and A. S. Nielsen (2003), Full spectrum inversion of radio occultation signals, *Radio Sci.*, *38*(3), 1040, doi:10.1029/2002RS002763.

Kirchengast, G., A. K. Steiner, U. Foelsche, L. Kornblueh, E. Manzini, and L. Bengtsson (2000), Spaceborne climate change monitoring by GNSS occultation sensors, paper presented at 11th Symposium on Global Change Studies, Am. Meteorol. Soc., Long Beach, Calif.

Kirchengast, G., J. Fritzer, and J. Ramsauer (2002), End-to-end GNSS occultation performance simulator version 4 (EGOPS4) software user manual (overview and reference manual), *Tech. Rep. ESA/ESTEC-3/2002*, Inst. for Geophys., Astrophys., and Meteorol., Univ. of Graz, Graz, Austria.

Kursinski, E. R., et al. (1996), Initial results of radio occultation of Earth's atmosphere using the global positioning system, *Science*, *271*, 1107–1110.

Kursinski, E. R., G. A. Hajj, J. T. Schofield, R. P. Linfield, and K. R. Hardy (1997), Observing Earth's atmosphere with radio occultation measurements using the Global Positioning System, *J. Geophys. Res.*, *102*(D19), 23,429–23,465.

Ladreiter, H. P., and G. Kirchengast (1996), GPS/GLONASS sensing of the neutral atmosphere: Model independent correction of ionospheric influences, *Radio Sci.*, *31*, 877–891.

Leitinger, R., and G. Kirchengast (1997a), Easy to use global and regional models—A report on approaches used in Graz, *Acta Geod. Geophys. Hung.*, *32*, 329–342.

Leitinger, R., and G. Kirchengast (1997b), Inversion of the plasma signal in GNSS occultations—Simulation studies and sample results, *Acta Geod. Geophys. Hung.*, *32*, 379–394.

Leroy, S. S., and G. R. North (2000), The application of COSMIC to global change research, *Terr. Atmos. Oceanic Sci.*, *11*(1), 187–210.

Loiselet, M., N. Stricker, Y. Menard, and J.-P. Luntama (2000), GRAS—MetOp's GPS-based atmospheric sounder, *ESA Bull.*, *102*, 38–44.

Lusignan, B., G. Modrell, A. Morrision, J. Pomalaza, and S. G. Ungar (1969), Sensing the Earth's atmosphere with occultation satellites, *Proc. IEEE*, *4*, 458–467.

Palmer, P. I., J. J. Barnett, J. R. Eyre, and S. B. Healy (2000), A nonlinear optimal estimation method for radio occultation measurements of temperature, humidity, and surface pressure, *J. Geophys. Res.*, *105*(D13), 17,513–17,525.

Randel, W., et al. (2003), The SPARC intercomparison of middle atmosphere climatologies, *Stratos. Process. Role Clim. Newsl.*, *20*, 10–15.

Rieder, M. J., and G. Kirchengast (2001), Error analysis and characterization of atmospheric profiles retrieved from GNSS occultation data, *J. Geophys. Res.*, *106*(D23), 31,755–31,770.

Rocken, C., et al. (1997), Analysis and validation of GPS/MET data in the neutral atmosphere, *J. Geophys. Res.*, *102*(D25), 29,849–29,866.

Rocken, C., Y. Kuo, W. S. Schreiner, D. Hunt, S. Sokolovskiy, and C. McCormick (2000), COSMIC system description, *Terr. Atmos. Oceanic Sci.*, *11*(1), 21–52.

Rodgers, C. D. (2000), *Inverse Methods for Atmospheric Sounding: Theory and Practice*, World Sci., Hackensack, N. J.

Roeckner, E., L. Bengtsson, J. Feichter, J. Lelieveld, and H. Rodhe (1999), Transient climate change simulations with a coupled atmosphere-ocean GCM including the tropospheric sulfur cycle, *J. Clim.*, *12*, 3004–3032.

Silvestrin, P., R. Bagge, M. Bonnedal, A. Carlström, J. Christensen, M. Hägg, T. Lindgren, and F. Zangerl (2000), Spaceborne GNSS radio occultation instrumentation for operational applications, *Proceedings of 13th ION-GPS Meeting 2000*, Salt Lake City, Utah.

Sokolovskiy, S. (2003), Effect of superrefraction on inversions of radio occultation signals in the lower troposphere, *Radio Sci.*, *38*(3), 1058, doi:10.1029/2002RS002728.

Sokolovskiy, S., and D. Hunt (1996), Statistical optimization approach for GPS/Met data inversions, paper presented at URSI GPS/Met Workshop, Int. Union of Radio Sci., Tucson, Arizona.

Spilker, J. J. (1980), GPS signal structure and performance characteristics, in *Global Positioning System*, edited by P. M. Janiczek, pp. 29–54, Inst. of Navig., Washington, D. C.

Steiner, A. K., and G. Kirchengast (2004), Ensemble-based analysis of errors in atmospheric profiles retrieved from GNSS occultation data, in *Proceedings of 1st Int'l Workshop on Occultations for Probing Atmosphere and Climate (OPAC-1)*, pp. 149–160, Springer, New York.

Steiner, A. K., G. Kirchengast, and H. P. Ladreiter (1999), Inversion, error analysis and validation of GPS/MET occultation data, *Ann. Geophys.*, *17*, 22–138.

Steiner, A. K., G. Kirchengast, U. Foelsche, L. Kornblueh, E. Manzini, and L. Bengtsson (2001), GNSS occultation sounding for climate monitoring, *Phys. Chem. Earth, Part A*, *26*, 13–124.

Syndergaard, S. (2000), On the ionosphere calibration in GPS radio occultation measurements, *Radio Sci.*, *35*, 865–883.

Turchin, V. F., and V. Z. Nozik (1969), Statistical regularization of the solution of incorrectly posed problems, *Phys. Atmos. Ocean*, *5*, 14–18.

von Engeln, A., G. Nedoluha, G. Kirchengast, and S. Bühler (2003), One-dimensional variational (1-D Var) retrieval of temperature, water vapor, and a reference pressure from radio occultation measurements: A sensitivity analysis, *J. Geophys. Res.*, *108*(D11), 4337, doi:10.1029/2002JD002908.

Vorob'ev, V. V., and T. G. Krasil'nikova (1994), Estimation of the accuracy of the atmospheric refractive index recovery from Doppler shift measurements at frequencies used in the NAVSTAR system, *Phys. Atmos. Ocean*, *29*, 602–609.

Ware, R., et al. (1996), GPS sounding of the atmosphere from low Earth orbit: Preliminary results, *Bull. Am. Meteorol. Soc.*, *77*, 19–40.

Wickert, J., et al. (2001), Atmosphere sounding by GPS radio occultation: First results from CHAMP, *Geophys. Res. Lett.*, *28*, 3263–3266.

Wickert, J., T. Schmidt, G. Beyerle, R. König, C. Reigber, and N. Jakowski (2004), The radio occultation experiment aboard CHAMP: Operational data analysis and validation of vertical atmospheric profiles, *J. Meteorol. Soc. Jpn.*, *82*, 381–395.

Yunck, T. P., G. F. Lindal, and C. H. Liu (1988), The role of GPS in precise Earth observation, paper presented at Position, Location, and Navigation Symposium, IEEE, Orlando, Fla., 29 Nov. to 2 Dec.

Yunck, T. P., C. Liu, and R. Ware (2000), A history of GPS sounding, *Terr. Atmos. Oceanic Sci.*, *11*(1), 1–20.

A. Gobiet and G. Kirchengast, Institute for Geophysics, Astrophysics, and Meteorology, University of Graz, Universitaetsplatz 5, Graz A-8010, Austria. (andreas.gobiet@uni-graz.at)